

## **General Disclaimer**

### **One or more of the Following Statements may affect this Document**

- This document has been reproduced from the best copy furnished by the organizational source. It is being released in the interest of making available as much information as possible.
- This document may contain data, which exceeds the sheet parameters. It was furnished in this condition by the organizational source and is the best copy available.
- This document may contain tone-on-tone or color graphs, charts and/or pictures, which have been reproduced in black and white.
- This document is paginated as submitted by the original source.
- Portions of this document are not fully legible due to the historical nature of some of the material. However, it is the best reproduction available from the original submission.



SPACE AND COMMUNICATIONS GROUP

---

# FINAL REPORT

## NASA WELDING ASSESSMENT PROGRAM

---

(NASA-CR-175512) NASA WELDING ASSESSMENT  
PROGRAM Final Report (Hughes Aircraft Co.)  
44 p HC A03/MF A01 CSCL 13H

N85-21661

Unclas  
G3/37 19382

JPL Contract No. 956038

December 1984



# **FINAL REPORT**

# **NASA WELDING ASSESSMENT PROGRAM**

**Prepared for:**

**JET PROPULSION LABORATORY  
CALIFORNIA INSTITUTE OF TECHNOLOGY  
4800 Oak Grove Drive, Pasadena, California 91109**

**JPL Contract No. 956038**

**December 1984**

This work was performed for the Jet Propulsion Laboratory, California Institute of Technology sponsored by the National Aeronautics and Space Administration under Contract NAS7-918

**Prepared By: E. J. Stofel**

This document contains information prepared by Hughes Aircraft Company under JPL sub-contract. Its content is not necessarily endorsed by the Jet Propulsion Laboratory, California Institute of Technology, or its sponsors.



## ACKNOWLEDGMENT

This author thanks the Hughes personnel who have contributed to this project: E. Browne, Jr., who was the engineer in charge of the ultrasonic welding, and R. Ritter, who designed and fabricated the Kevlar substrate. Their insight into fabrication processes used on many present spacecraft ensured that the module design selected for testing is representative of a production approach using readily available materials and processes. The author also acknowledges the extensive contributions made by Spectrolab, Inc., as the major subcontractor in this project. N. Mardesich and M. Gillanders of Spectrolab made substantial contributions to the design of the modules as well as supervising solar cell manufacturing, parallel gap welding, and the soldering of Spectrolab's portion of the modules and coupons. Technical discussions with J. Scott-Monck of the Jet Propulsion Laboratory and with C. Bararona, J. Bozek, and R. Hart of the NASA Lewis Research Center also contributed significantly to the establishment of test guide lines.

## ABSTRACT

A long duration test has been conducted for comparing various methods of attaching electrical interconnects to solar cells for near earth orbit spacecraft. Representative solar array modules have been thermally cycled for 36,000 cycles between  $-80^{\circ}$  and  $+80^{\circ}$ C on this JPL and NASA Lewis Research Center sponsored work. This test simulates the environmental stress of more than 6 years on a near earth spacecraft as it cycles in and out of the earth's shadow. Evaluations of the integrity of these modules were made by visual and by electrical examinations before starting the cycling and then at periodic intervals during the cycling tests.

Modules included examples of parallel gap and of ultrasonic welding, as well as soldering, which were fabricated by the Space and Communications Group of Hughes Aircraft Company and by Spectrolab, a subsidiary of Hughes. The materials and fabrication processes are state of the art, suitable for forming large solar arrays of spacecraft quality. The modules survived this extensive cycling without detectable degradation in their ability to generate power under sunlight illumination.

PRECEDING PAGE BLANK NOT FILMED

## CONTENTS

	Page
1. INTRODUCTION	1
2. MODULE DESCRIPTION	5
2.1 Module Overview	5
2.2 Materials	12
2.3 Welding Description	14
2.4 Strength of Welds	20
2.5 Coupons	21
3. THERMAL TESTING	27
4. CONCLUSIONS	37
5. NEW TECHNOLOGY	39

~~PRECEDING~~ PRECEDING PAGE BLANK NOT FILMED

## ILLUSTRATIONS

	<b>Page</b>	
1	Module Overview	6
2	Ultrasonically Welded Module Front	7
3	Ultrasonically Welded Module Back	7
4	Parallel Gap Welded Module Front	8
5	Parallel Gap Welded Module Back	8
6	Module Cross Section	10
7	Photovoltaic Response of Representative Solar Module at 28°C, AM0 Illumination	11
8	Ultrasonic Weld Station Schematic	15
9	Ultrasonic Weld Front	15
10	Ultrasonic Weld Cross Section	16
11	Ultrasonic Weld Detail	16
12	Parallel Gap Weld	18
13	Parallel Gap Weld Cross Section	18
14	SCG Pull Tab Configuration	22
15	Ultrasonic Weld Pull Tabs	22
16	Spectrolab Pull Tab Configuration	24
17	Parallel Gap Weld Pull Tab	24
18	Parallel Gap Welded Cell Front	26
19	Parallel Gap Welded Cell Back	26
20	Sunlight Simulation Testing Module Fixture	28
21	Thermal Cycling Equipment Schematic	30
22	Thermal Cycling Machine	30
23	Module Test Tray	31
24	Module Test Tray Cross Section	31
25	Partially Assembly Module Tray	32

## TABLES

		<b>Page</b>
1	Test Requirements	2
2	Components for Modules	9
3	Component Weights for 9-Cell Modules	10
4	Array Power Density Performance	11
5	Pull Test of Ultrasonic Bonds	22
6	Pull Test of Parallel Gap Bonds	23
7	Fill Factors at 28°C for 12 Modules During Thermal Test	24
8	Fill Factors at 80°C for 12 Modules During Thermal Test	35

## 1. INTRODUCTION

Future spacecraft are expected to have longer operating life than has been typical of past spacecraft. NASA is now giving serious consideration to missions that will operate for up to 10 years in near earth orbit. During this time, solar arrays will be subjected to as many as 60,000 thermal cycles as they pass in and out of the earth's shadow. Since any solar array is fabricated from a variety of materials having differing coefficients of thermal expansion, this thermal cycling will produce repeated cycles of strain and stress within the array. If sufficiently severe, the resulting fatigue will rupture the continuity of the delicate electrical interconnects between cells. The loss of electrical continuity will mean loss of electrical power to the spacecraft.

NASA has embarked recently on an experimental investigation of the extent to which such thermal cycling poses a threat to the long duration operation of solar arrays. The comparison between welded interconnects and soldered interconnects is receiving particular attention. The metallurgical simplicity inherent in welds gives them a theoretical advantage over the more massive, multimetal composite structure of soldered joints. However, practical space experience with welded interconnects operating for many years in near earth orbit does not exist. NASA, therefore, is assessing the present state of the art of welded and of soldered solar cell interconnects by sponsoring a series of laboratory tests that are cycling representative solar array modules under conditions that thermally simulate long duration exposure in space. This study is one of these NASA sponsored investigations.

The procedure for this investigation is as follows:

- 1) Review candidate solar array materials and fabrication processes as they exist today.

- 2) Select an optimum combination of these state of the art materials and processes to achieve a lightweight solar array design that emphasizes long term tolerance of repeated thermal cycling.
- 3) Fabricate representative small modules of the selected design.
- 4) Measure electrical performance of these modules.
- 5) Subject the modules to extended, repetitive thermal cycling.
- 6) Periodically interrupt the cycling long enough to remeasure electrical performance to detect any thermally induced electrical degradation and record it as a function of the increasing number of cycles.

The general configurations of the test modules and of the test parameters, specified by the Jet Propulsion Laboratory acting in behalf of NASA, are summarized in Table 1. These test conditions are similar to conditions that NASA specified for concurrent companion solar array cycling investigations sponsored by NASA at Lockheed Missiles and Space Company and at TRW. The results of these three investigations, each conducted independently, provide a valuable survey of the durability of state of the art solar arrays.

TABLE 1. TEST REQUIREMENTS

Parameter	Comment
Simultaneous testing of at least 8 modules	3 SCG welded modules 3 Spectrolab welded modules 1 SCG soldered module 1 Spectrolab soldered module
Nominal temperature limits	+80°C to -80°C
Uniformity over test plane at temperature limits	±5°C
Atmosphere	Dry N <sub>2</sub>
Thermal cycles	36,000
Scheduled inspection cycles	0 500 1,000 2,000 4,000 8,000 12,000 24,000 30,000 36,000

The present study was conducted by the Space and Communications Group (SCG) of Hughes Aircraft Company and by Spectrolab, a subsidiary of Hughes. Although both organizations are part of Hughes, they operate independently under two separate profit centers with differing background experience on solar array fabrication. During the initial phase of this investigation, it became apparent that this difference was leading to alternative design approaches. Rather than eliminate one approach in favor of the other, Hughes decided to try both. The cycling test would then be used to determine whether one approach excelled over the other. The approach selected by SCG features a cell to cell electrical interconnect that is as thin and compliant as possible (0.011 mm thick silver mesh), accommodating in a low stress manner the differences of thermal expansion and contraction of differing adjacent materials. The approach selected by Spectrolab features a cell interconnect material that matches the thermal expansion of silicon (silver plated Invar or molybdenum), minimizing stress by minimizing expansion differences. The SCG interconnect lends itself best to ultrasonic welding between the interconnect and cell, demonstrated earlier in the thin cell welding part of this JPL contract.\* The Spectrolab interconnect bonds best to a cell by parallel gap welding. Both types of interconnects can be readily soldered. For all other components of the solar array modules, agreement was made to use materials and processes in common.

---

\*E. J. Stofel, Ultrasonic Seam Welding on Thin Silicon Solar Cells, Final Report, for JPL Contract No. 956038, Hughes Aircraft Company SCG 820419R, June 1982.



## 2. MODULE DESCRIPTION

### 2.1 MODULE OVERVIEW

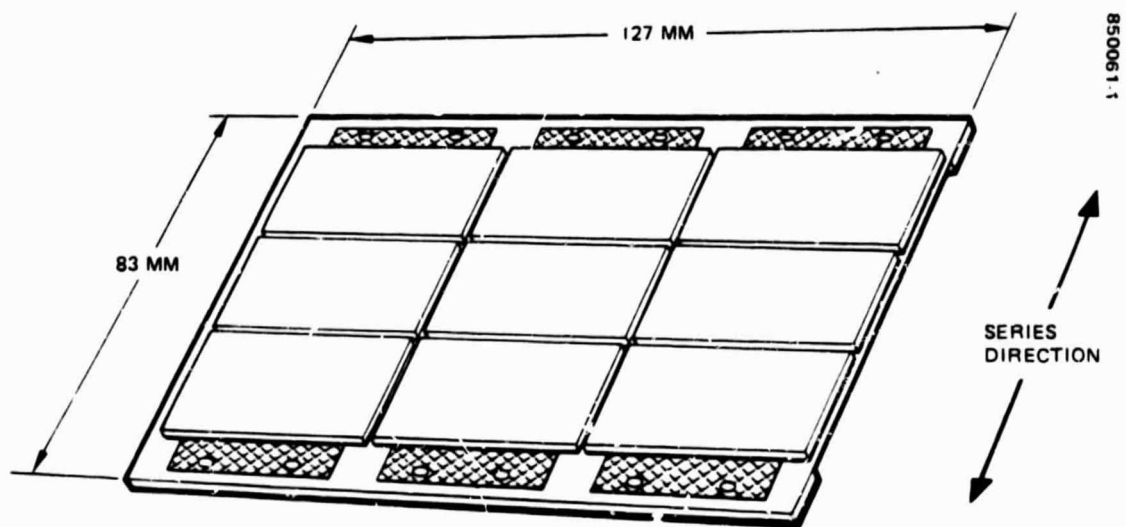
The modules tested in this investigation have the configuration depicted schematically in Figure 1. Figures 2 through 5 are examples. All modules are similar except for differing methods of forming the interconnects. Comparison of performance after cycling is a comparison of the durability of the examined types of interconnects.

The module components, which are space quality, are summarized in Table 2. Their arrangement is shown in Figure 6, and the weights are given in Table 3. Figure 7 presents the photovoltaic power response of a representative module. The NASA electrical performance requirements for the modules were exceeded as summarized in Table 4.

State of the art fabrication processes were used to assemble these modules. The cells, covers, and adhesives are typical of those used extensively in space. Soldering is also commonly used on spacecraft arrays. While the welding on these modules has not been used by SCG or Spectrolab in space, extensive laboratory development has been performed by both organizations with results demonstrated and evaluated on several thousand cells. The welding processes used for fabricating the samples of this present thermal cycling program are those optimized for anticipated space application.

Twenty-three modules were fabricated: 9 welded and 3 soldered by SCG and 7 welded and 4 soldered by Spectrolab. The slight differences, noted in Table 4 in area and in mass densities between the ultrasonic and the parallel gap welded modules, are caused by the differences of interconnect thickness and flexibility. Not only was the interconnect used on the ultrasonically welded modules lighter in weight than the interconnect on the parallel gap welded modules, its thinness also permitted less adhesive to be used between the cover and the cell (Table 3). On the other hand, the rigidity of the interconnect used with parallel gap welding allowed the cell to cell spacing gap to be

held consistently to a smaller value than for the more flexible, ultrasonically welded interconnect which resulted in a higher areal density with the parallel gap welded modules (Table 4). In all other respects, the modules were similar.



9 SILICON SOLAR CELLS, 21.1 x 40.3 x 0.2 MM.  
INTERCONNECTED 3 IN PARALLEL BY 3 IN SERIES

FIGURE 1. MODULE OVERVIEW

ORIGINAL PAGE IS  
OF POOR QUALITY

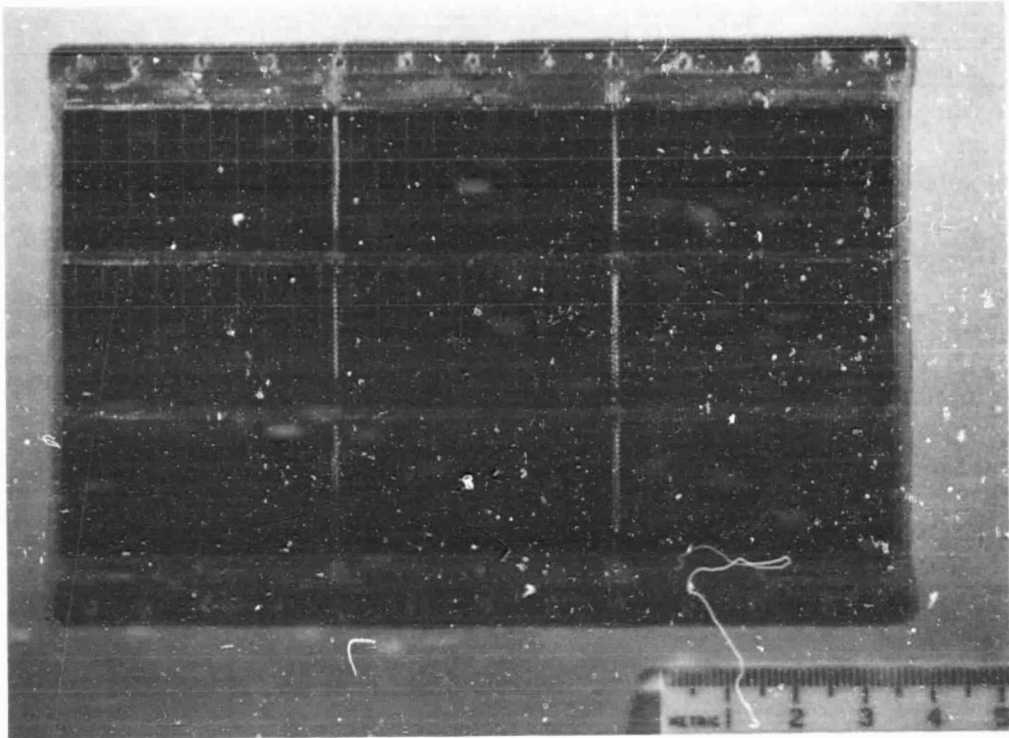


FIGURE 2. ULTRASONICALLY WELDED MODULE FRONT

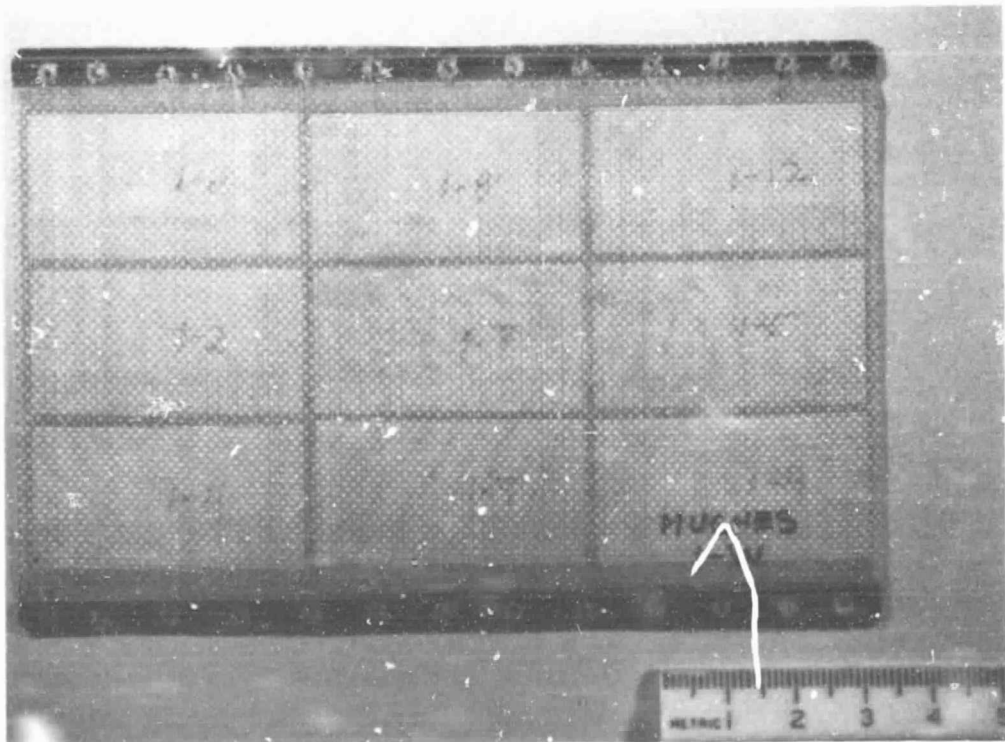


FIGURE 3. ULTRASONICALLY WELDED MODULE BACK

850061-4

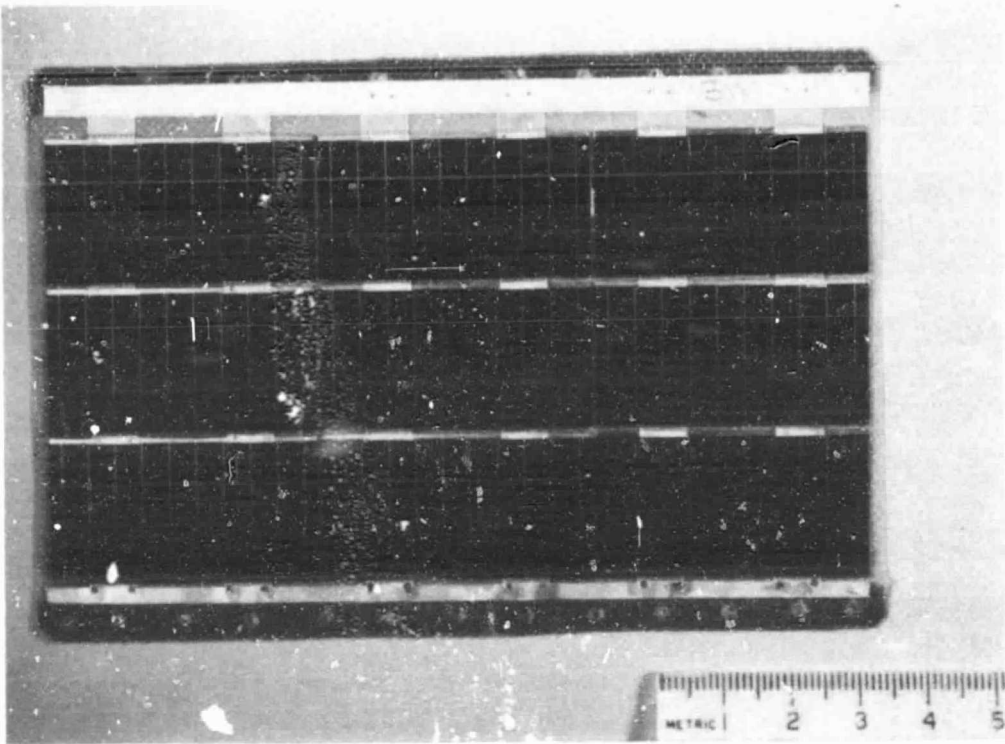


FIGURE 4. PARALLEL GAP WELDED MODULE FRONT

850061-5

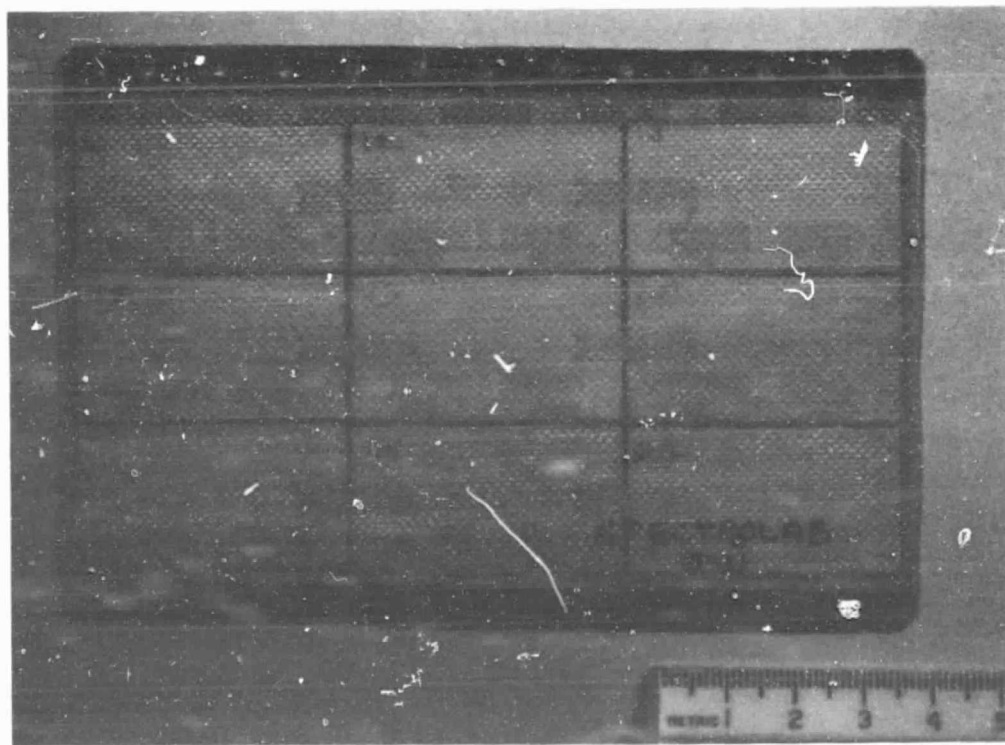


FIGURE 5. PARALLEL GAP WELDED MODULE BACK

TABLE 2. COMPONENTS FOR MODULES

Component	Requirement
Solar cells	14% efficient Silicon 10 ohm-cm P base with dual antireflective coating (DAR), back surface reflector (BSR), and back surface Field (BSF). 21.1 x 40.3 x 0.20 mm
Covers	C7940 silica glass MgF <sub>2</sub> antireflective overcoating Ultraviolet reflecting undercoating 21.1 x 40.3 x 0.15 mm
Cover to cell adhesive	DC 93-500 silicone
Interconnects	
SCG ultrasonic welding	0.011 mm thick pure silver foil Mesh configuration Chemically etched
Spectrolab parallel gap welding	0.035 mm thick Invar with 0.007 mm thick silver plate on each side Mesh configuration Chemically etched
SCG soldering	0.011 mm thick pure silver foil Mesh configuration Chemically etched
Spectrolab soldering	0.030 mm thick molybdenum with 0.005 thick silver plate on each side Mesh configuration Chemically etched
Solder	38% lead 2% silver 60% tin Screen printed pads on Spectrolab soldered modules
Cell to substrate adhesive	DC 93-500 silicone
Substrate	Kevlar fabric, rigidized with epoxy resin

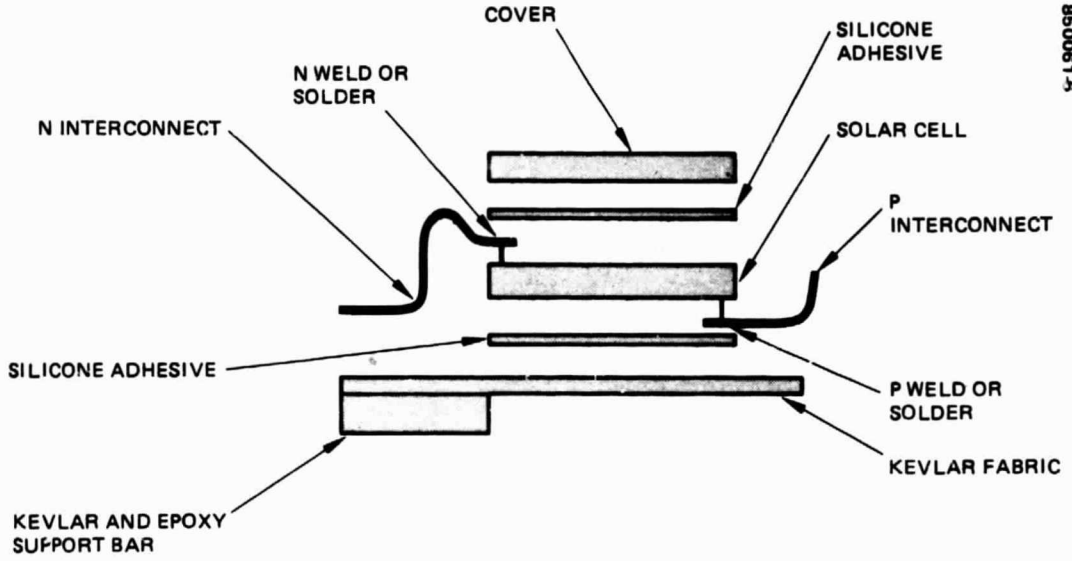


FIGURE 6. MODULE CROSS SECTION

TABLE 3. COMPONENT WEIGHTS FOR 9-CELL MODULES

Component	Ultrasonic, gm	Parallel Gap, gm
Cells, 21.1 x 40.3 x 0.20 mm silicon with DAR, BSR, BSF	3.80	3.80
Covers, 21.1 x 40.3 x 0.15 mm C7940 silica	2.82	2.82
Cover adhesive, DC-93-500	0.30	0.70
Series interconnects	0.26	0.38
Parallel interconnects	0.09	0.18
End connectors	0.09	0.30
Cell to substrate adhesive, DC-93-500	0.40	0.40
Substrate, Kevlar	<u>1.35</u>	<u>1.35</u>
Total	9.1	9.9

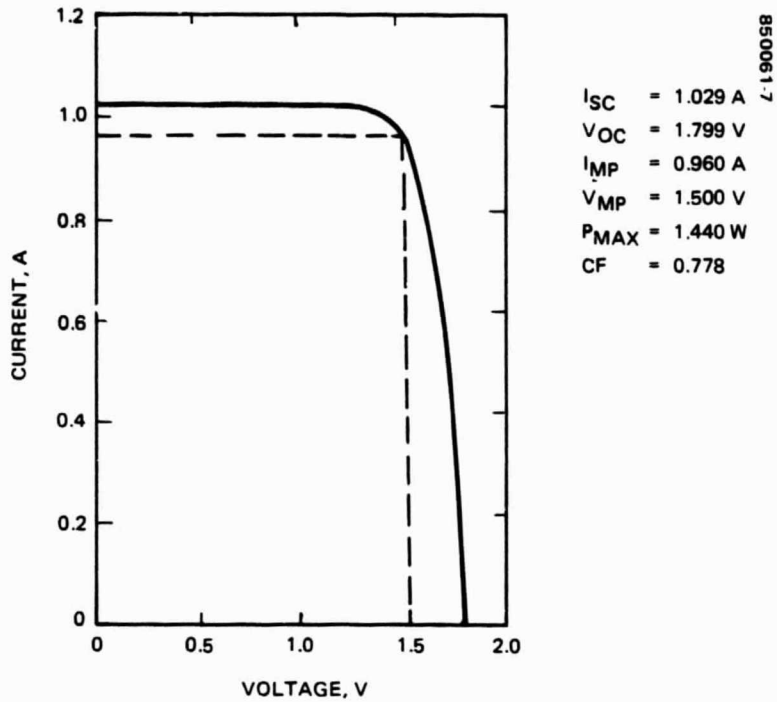


FIGURE 7. PHOTOVOLTAIC RESPONSE OF REPRESENTATIVE SOLAR MODULE AT 28°C, AMO ILLUMINATION

TABLE 4. ARRAY POWER DENSITY PERFORMANCE

Parameter	Requirement	Achievement	
		Ultrasonic	Parallel Gap
Areal density, $w/m^2$	$\geq 140$	173	178
Mass density, $w/kg$	$\geq 90$	169	157
Achievement:			
Module power at 28°C, AMO, W		1.44	1.44
Active Module area, $mm^2$		8343	8073
Weight of active area, gm		8.5	9.1
Weight of total module, gm		9.1	9.9

## 2.2 MATERIALS

For all modules, the selected solar cells were of Spectrolab K6700 type. These cells have a shallow, planar N on P junction, a front dual antireflective (DAR) coating, an aluminum rich back surface field (BSF), and an aluminum back surface reflector (BSR). The contact metalization is the conventional titanium-palladium-silver combination. These cells have an efficiency of 14 percent at 28°C under air mass zero (AM0) solar illumination. This type is already in standard production and would be readily available for large area solar arrays. The use of a back surface field is an appropriate means of achieving high power density since at near earth orbits the radiation environment is relatively benign. The enhanced power achieved with the BSF would therefore not be lost as a result of radiation damage. The planar front surface was selected over the nominally more efficient (at standard 28°C) sculptured surface because the planar cell has a lower solar absorptivity which produces a relatively cool operating panel. The cooler operation enhances power output in orbit.

The coverglass for the cells is a space qualified type manufactured by the Optical Coating Laboratories, Inc. (OCLI). The base material is Corning 7940 fused silica. Both bottom and top surfaces are polished flat. The top surface has a magnesium fluoride coating for antireflection of visible light. The bottom surface has OCLI's multilayer, ultraviolet reflective coating. This coverglass is used routinely on solar arrays assembled by Hughes and by several other spacecraft manufacturers.

The covers were bonded to the front of the solar cells with DC-93-500 clear silicone adhesive which is used conventionally to bond covers to cells on all flight programs at SCG and at Spectrolab. Alignment of covers over the cells was achieved using mechanical fixtures, as used for present flight hardware. The coverglass covered each cell completely (including the front contact area). Therefore, all cells had their interconnects attached to the front contact, either by welding or by soldering, prior to bonding the coverglass to the cell. The subassembly resulting was a covered, interconnected cell (CIC). This type of subassembly, with welded interconnects, is used on the solar array for Intelsat VI. SCG also is planning to use this assembly configuration on future welded solar arrays. This approach differs slightly from present practice on SCG soldered solar arrays wherein covers are bonded to the front of the cells prior to soldering the interconnect to the front contact. For this latter configuration, the covers are slightly undersize so that the front contact is exposed for subsequent soldering.



There is no apparent reason why future soldered arrays could not just as well be assembled using the CIC configuration. For the SCG modules of this test program, solder was applied by hand. For the Spectrolab modules, solder was applied as screen printed pads.

The substrate for all modules was formed from a sheet of Kevlar woven fabric. Prior to bonding cells to this fabric, it was impregnated with a small amount of liquid epoxy. The fabric was held flat while the epoxy cured. This process produced a substrate with in-plane rigidity but with out-of-plane flexibility, similar to a sheet of heavy-weight paper. It no longer had the flexibility and drape of the untreated fabric. The stiffness imparted by the epoxy made it practical to bond cells to it en masse. There was no possibility of local distortion of the interconnect during bonding which would have occurred had the fabric maintained a clothlike drape. It was as easy to handle this epoxy impregnated Kevlar as it would have been to handle a sheet of Kapton, a more traditional material for substrate use on lightweight solar arrays. Kevlar has the advantage over Kapton of being more tear resistant, a lower coefficient of expansion, and a surface sufficiently porous to readily provide a strong, interlocking bond to the silicone adhesive that was used to bond the cells to the substrate.

The electrically interconnected solar cell strings were bonded to the substrate using DC-93-500 silicone adhesive, a material selected from among several candidates. An alternative candidate, considered in detail, was precut pieces of uncured sheet epoxy. The intent with this epoxy material was to limit the adhesive to a selected area of the back of each cell so that no adhesive would flow into the interconnect. By keeping the interconnect free of any restraining epoxy, the thin mesh style interconnect could flex in a low stress, uninhibited manner to accommodate thermal expansion and contraction most readily. However, the application of precut adhesive film was found to be less convenient as a mass production method than the simple method of spreading a thin, uniform layer of silicone adhesive onto the substrate. Furthermore, the use of epoxy film, which was precut to be small enough to avoid the interconnect area on the back of the cells, also significantly reduced the area of heat transfer between the cell and the back of the solar array. The array would therefore have operated at a higher, less efficient temperature.

Of the various candidates for a silicone adhesive, DC-93-500 was selected because its transparency allows visual inspection of the interconnect before and after

cycling even for those modules containing sufficient adhesive to engulf the interconnects. Furthermore, this material is low in outgassing and is completely acceptable for any flight array. Indeed, besides being the adhesive used regularly between covers and cells, it has already been used to bond solar cells to substrates on a few past spacecraft. For fabricating most modules of this test project, the amount of DC-93-500 applied between the cells and substrate was controlled to a low level, an amount insufficient to allow excess accumulation between the cells at the cell interconnects. However, to test for the effect on thermal cycle endurance that an excess would cause if it became an accidental manufacturing variable under future mass production, sufficient adhesive was intentionally added on a few modules so that excess adhesive arose between cells, covering the cell interconnects. Thus, comparing the durability of modules with the two configurations of adhesive provided information as to whether the presence or absence of adhesive embedment of interconnects affects the longevity of the interconnect under extended thermal cycling.

### 2.3 WELDING DESCRIPTION

The ultrasonic welds were made using a rotating, seam welding machine. This machine and its operation were described in a previous report of this JPL contract and at the Sixteenth IEEE Photovoltaic Specialist Conference.\* The principle of its operation is depicted in Figure 8. The ultrasonically active wheel produces a track of weld spots (see Figure 9) as it rolls over the mesh style interconnect foil. Such welding produces an intimate bond between the interconnect and the silver metallization on the solar cell. A photomicrograph of a metallurgical cross section of one of these weld spots is shown in Figure 10. There were 45 such bonds formed in parallel redundancy on the front of each cell and 45 on the back. The intimacy of the bond is emphasized in Figure 11, which shows a magnified view of the central part of Figure 10. The small void in the band of metal at the center of this figure provides an unusual opportunity to reveal the location of the interface between the applied interconnect and the original silver contact. The source of this void was a shallow depression that had existed on the surface of the silicon

\*E. J. Stofel, Ultrasonic Seam Welding on Thin Silicon Solar Cells, Final Report, for JPL Contract No. 956038, Hughes Aircraft Company SCG 820419R, June 1982. E.J. Stofel, E.R. Browne, R.A. Meese, and C.J. Vendura, "Welded Solar Cell Interconnection," 16th Photovoltaic Specialists Proceedings, 1982, pp. 45-50.

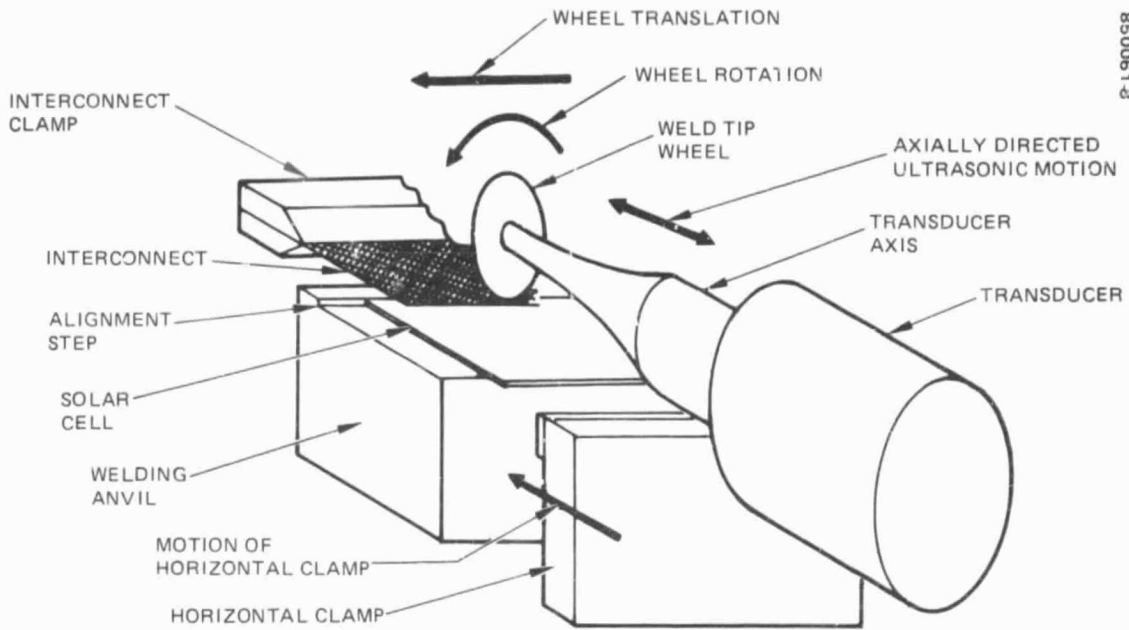


FIGURE 8. ULTRASONIC WELD STATION SCHEMATIC

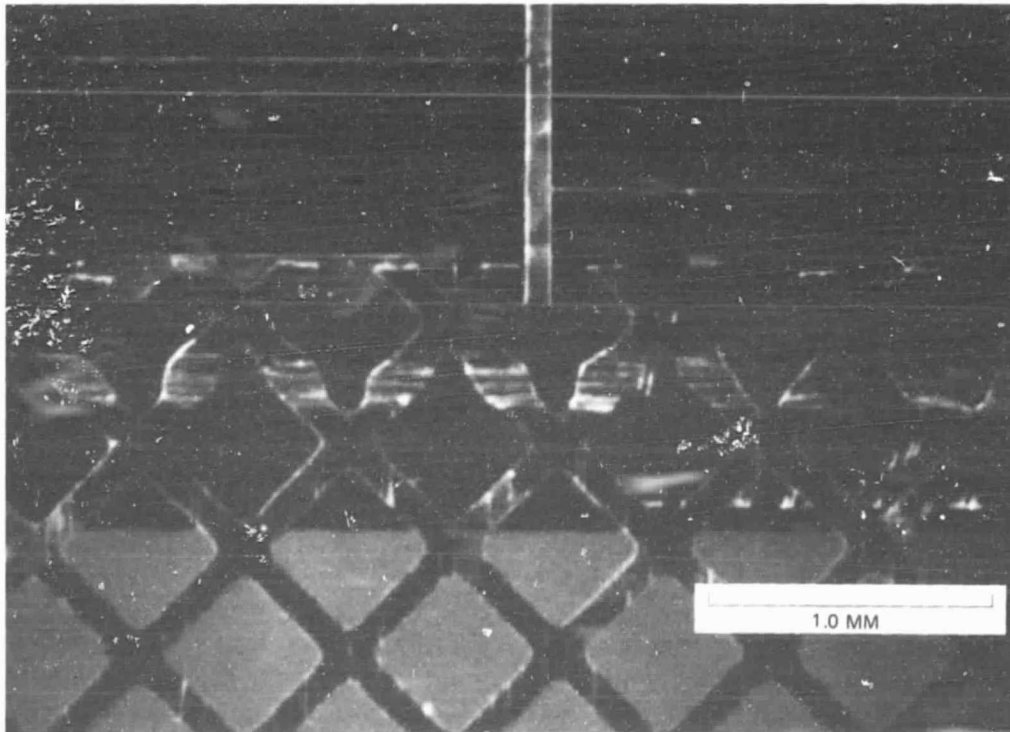


FIGURE 9. ULTRASONIC WELD FRONT

ORIGINAL PAGE IS  
OF POOR QUALITY

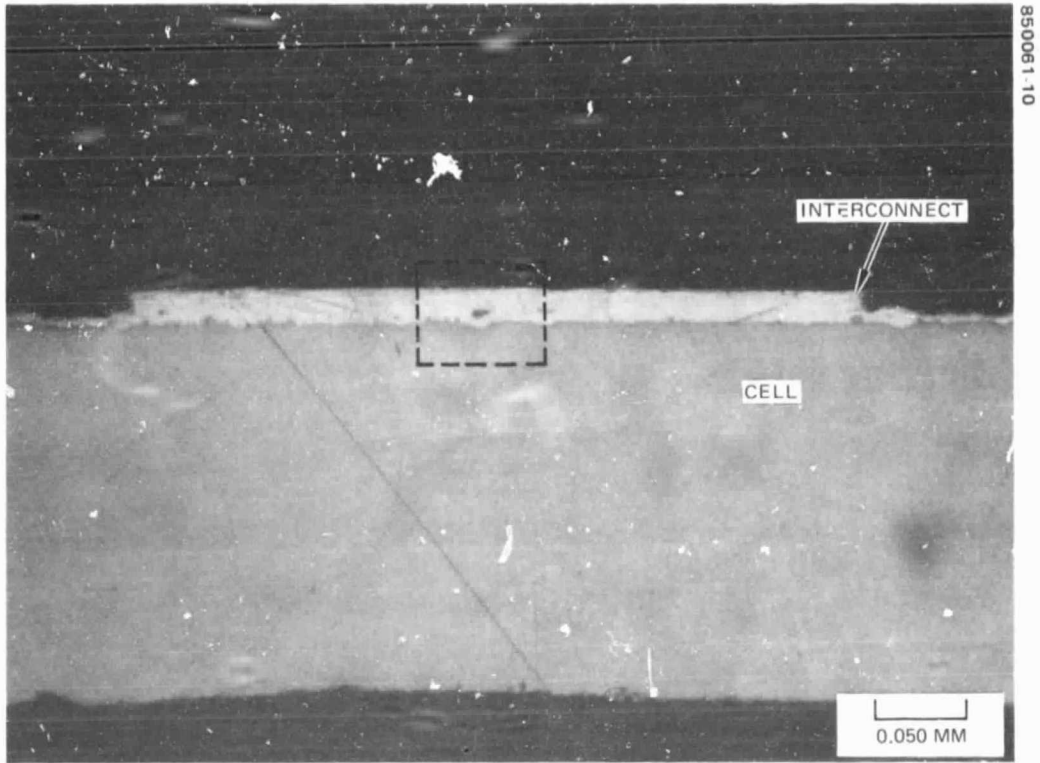


FIGURE 10. ULTRASONIC WELD CROSS SECTION

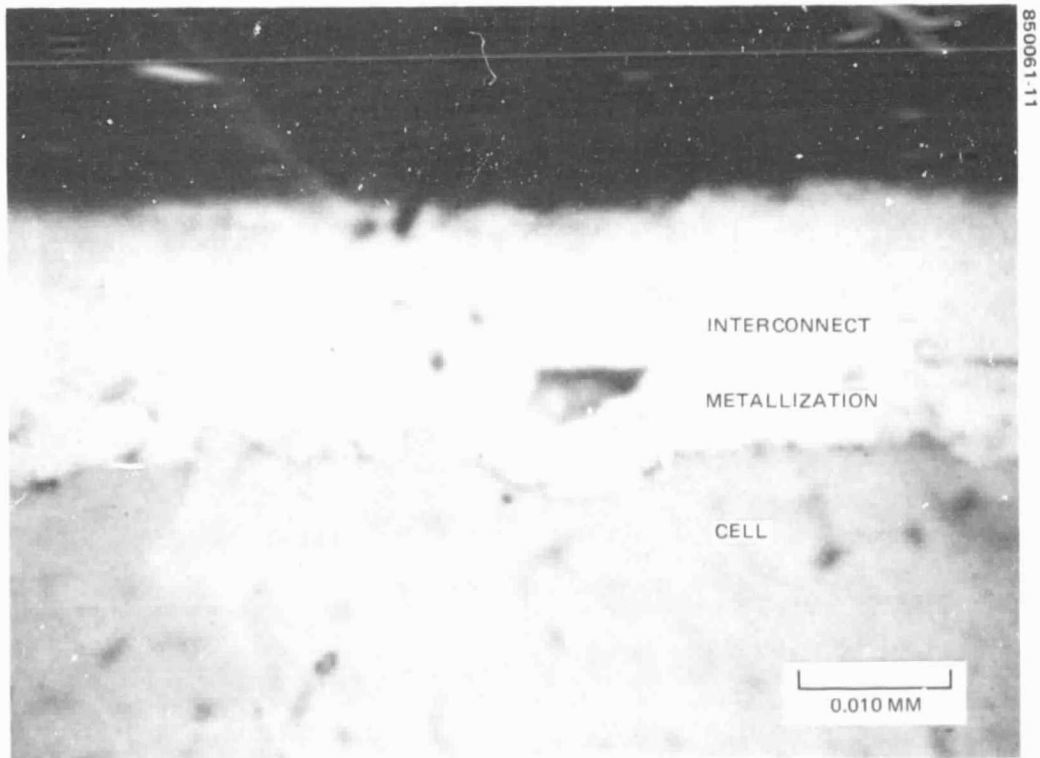


FIGURE 11. ULTRASONIC WELD DETAIL

prior to applying the silver front contact. The contact metallization, applied by the cell manufacturer, followed the contour of the silicon; therefore, it also had a shallow depression at this location. The subsequent ultrasonic welding of the interconnect to the cell did not deform the interconnect sufficiently to fill this depression. This depression thus remains as a visually distinct mark that not only reveals the location of the original interface between the interconnect and the cell contact, but by contrast with the material to the left and to the right, also emphasizes the metallurgical continuity across the weld interface that exists over the majority of the welded area.

The parallel gap welds were made by pressing two small, closely spaced electrodes against the top surface of the interconnect as it lay upon the cell contact. A pulse of current was conducted down one of the electrodes, through the interconnect material bridging the small gap between the electrodes, then up the other electrode. The current pulse produced sufficient localized heating in the interconnect to cause the interconnect to bond to the cell metallization in the interface region under the action of the high mechanical pressure applied by the electrodes. The size of the electrical pulse was carefully controlled to provide a temperature sufficiently near melting to ensure strong bonding while at the same time not overheating to a degree that would have produced extensive melting and loss of interconnect integrity. This parallel gap method has been a common welding process for several years on a variety of electrical circuits. Specifically, it has been the welding method most commonly used by several organizations for welding interconnects to solar cells, including several flight solar panels that have been constructed in Europe. A pair of weld spots from the present program is shown in Figure 12. A photomicrograph of a metallurgical cross section of one of these weld spots is shown in Figure 13. Eight such spots were used in parallel redundancy on the front of each cell and eight on the back.

The two types of welding methods, each with its distinctive interconnect, were chosen to provide emphasis on comparing two different approaches toward achieving long fatigue life. Either of these approaches must provide tolerance for two types of thermally induced stress. The first type occurs as a shear stress at the interface bond between the interconnect and the solar cell, the result of differing thermal coefficients of expansion between the metal interconnect and the underlying silicon. The second type of stress occurs from changes in cell to cell spacing caused by the difference in expansion between the substrate and the interconnect. This puts the interconnect alternately in tension and compression. Not only does this fatigue the portion of the

850061 12

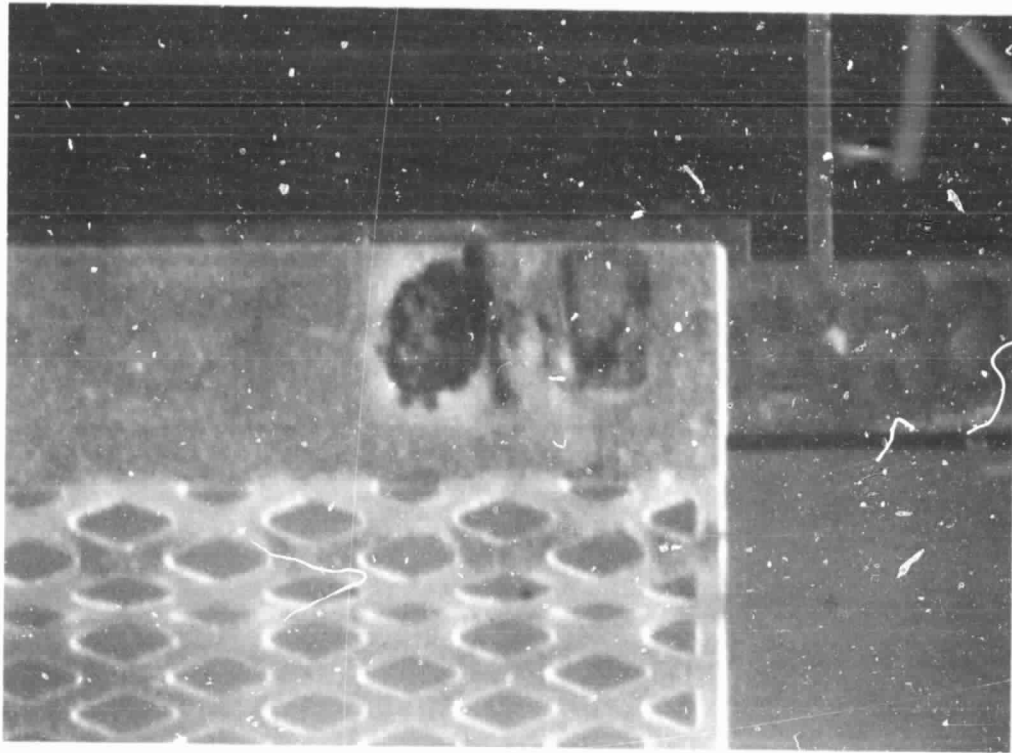


FIGURE 12. PARALLEL GAP WELD

850061 13

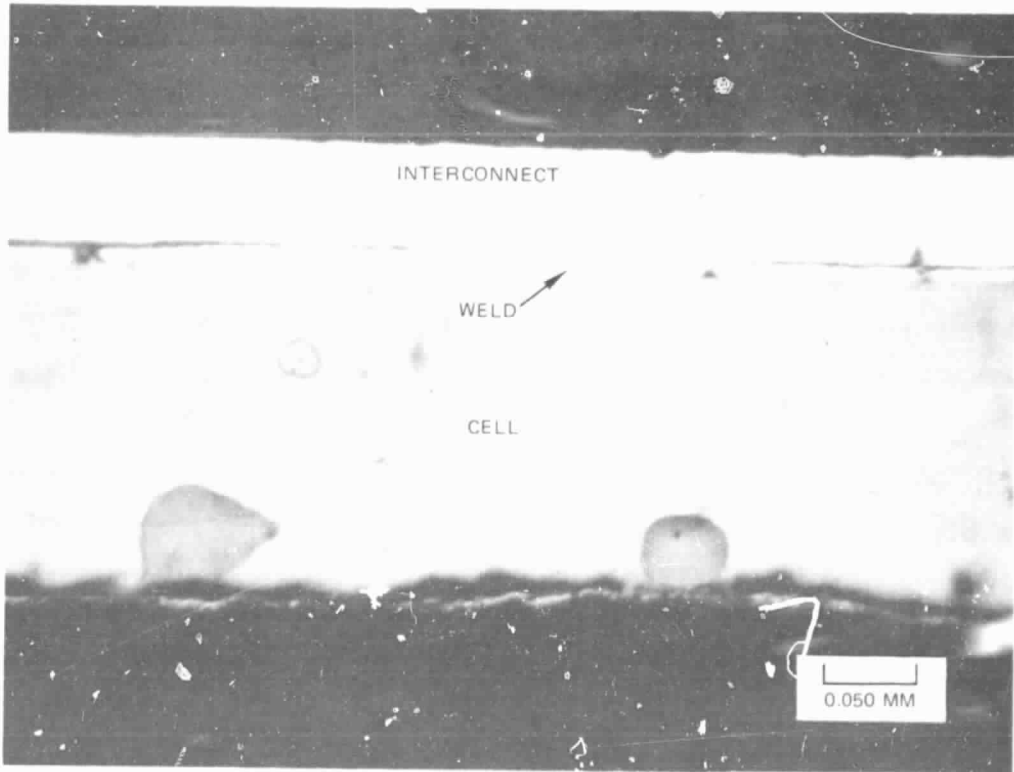


FIGURE 13. PARALLEL GAP WELD CROSS SECTION



interconnect bridging between cells, it also aggravates the shear stress acting on the bond line between the interconnect and the solar cell.

The ultrasonically welded modules feature a very compliant interconnect. The thinness of the foil (Figure 10) allows large deflections to occur in the out of plane loop (Figure 6) without producing large fatigue strain within the metal. The change in cell to cell spacing caused by expansion and contraction under thermal cycling therefore is accommodated without large bending stress in the interconnect nor large force being applied to the welded area. Thermally induced shear at the bond line also is kept small by having the metal thickness overlying the silicon as thin as possible, thus partially alleviating the problem of their differing coefficients of expansion. The relatively large holes in the diamond shaped mesh pattern (Figure 9) aid in providing compliance in the plane of the foil and retard tear propagation. The narrow strips of metal around the holes result in a large number of small weld areas. All act electrically in parallel redundancy; however, the compliancy of the mesh allows each weld area to be mechanically decoupled from its neighbors. The accidental debonding of one small weld area therefore does not cause propagation of debonding to adjacent weld areas.

Since silver is an excellent electrical conductor, this low cross section, highly compliant interconnect configuration is permitted without introducing significant series electrical resistance. Ultrasonic welding is a good production method of rapidly making many weld bonds to such thin material without the possibility of accidentally overheating and melting it.

The parallel gap welded modules feature an interconnect with a very low coefficient of thermal expansion, one approximately the same as the underlying silicon. By matching coefficients, the contact shear stress can be kept low over a range of operating temperatures. The parallel gap welded modules of this program use a silver plated Invar interconnect. The Invar provides the low expansion; the silver is required for adequate electrical conductivity. This combination is relatively thick (compare Figure 13 with Figure 10) since it is difficult to obtain thinner Invar foil. The resultant interconnect is much stiffer than the simple, thin silver interconnect. This stiffness is caused by the greater thickness and higher modulus of elasticity of Invar. The out of plane stress relief loop (Figure 6) thus does not provide much compliance within the Invar interconnect. To prevent large stress in the interconnect, the substrate, therefore, must also have a low thermal coefficient of expansion. Kevlar was chosen for this substrate.

## 2.4 STRENGTH OF WELDS

Prior to fabricating the thermal cycle test modules, tabs of representative interconnect material were welded to several sample cells to demonstrate the production readiness of both welding methods. The strength of these welds was evaluated by pulling the interconnect tabs to destruction. Four types of separation could occur:

- 1) Simple separation at weld interface between the interconnect and cell metallization.
- 2) Fracture of underlying silicon material.
- 3) Rupture of interconnect material immediately adjacent to the weld where the interconnect had been deformed by the welding process.
- 4) Plastic stretching of interconnect tab and its eventual rupture somewhere along the length of the tab away from the welded region.

If a large pull force was required to cause destruction, then no matter what its failure mode that weld was considered to have been of adequate strength for typical flight applications. If a small force caused destruction, then the different failure modes were indicative of different problems with welding. Type 1 failure, parting at the weld interface, could arise at a low force if insufficient energy had been delivered during welding which would leave an incomplete weld interface. Contaminated surfaces prior to welding could produce a similar result. Type 2 failure, rupture of the underlying silicon, could indicate the introduction of microcracks at the time of welding due to too much weld pressure or energy. Type 3 failure, rupture of the interconnect adjacent to the weld, arises when too much weld energy is used and the cross sectional area is greatly reduced due to extensive plastic deformation of the interconnect metal. Type 4 failure, plastic stretching of the interconnect, is not a failure mode associated with the weld. If stretching had occurred at an abnormally small force, it would have indicated a defect in the interconnect or an improperly aligned pull test.

For testing the ultrasonically welded cells, a mesh interconnect was first welded along the full width of the cell (as depicted in Figure 9) in the same manner that was used on the thermal cycle test modules and will be used on flight solar arrays. The mesh was then cut with a sharp razor blade into several parallel 3.0 mm wide tabs, each with



the dimensions indicated in Figure 14. Tabs prepared this way had welds that were representative of rolling seam welding, with each tab having four small, independent weld areas.

An example of the result obtained by pulling four adjacent tabs is presented in Figure 15. Two tabs failed by type 3, two by type 4. Table 5 summarized pull results of all tested ultrasonic welds. Some of these welds were pulled at an angle of  $45^{\circ}$  with respect to the plane of the front surface of the cell; the remainder were pulled normal to this plane. The  $45^{\circ}$  pull produces a combination of shear and peel at the weld; the  $90^{\circ}$  pull produces only peel. The former condition is closer to the stress that can be expected during normal handling of welded cell strings during array assembly operations. The latter condition makes a more sensitive distinction of strength variation among nominally similar welds. Most tests ended by breaking the interconnect from 60 to 80 grams, the inherent strength of the interconnect. Only at  $90^{\circ}$  did a portion of welds fail by peeling apart at the weld interface. These pull results indicate an optimum set of weld parameters had been used. If more weld energy or pressure had been used, there would have been fewer welds separating in  $90^{\circ}$  peel. However, the resultant greater deformation of the interconnect during the welding would have allowed some type 3 failures to occur at less than 60 grams. On the other hand, with less welding energy, more  $90^{\circ}$  peeling would have occurred. The observed type 4 failure of the interconnect is the desired result, since the interconnect was designed to have sufficient compliancy to accommodate movement with easy strain rather than resisting movement by developing high stress.

The front contact pull tab configuration for the parallel gap welded cells is depicted schematically in Figure 16. A photograph of a back contact pull tab is shown in Figure 17. Table 6 summarizes the pull tab results. Since these tabs are thick (see Figure 13) and therefore have intrinsically high strength, none of the tabs broke. Instead, separation occurred either at the weld interface or by fracturing the underlying silicon. Since destruction force was large for all welds, the tests showed that parallel gap welding produces strong bonds.

## 2.5 COUPONS

Twenty-four welded cell assembly coupons and 12 welded coupons also were fabricated and sent to the NASA Lewis Research Center for evaluation per their

ORIGINAL PAGE IS  
OF POOR QUALITY

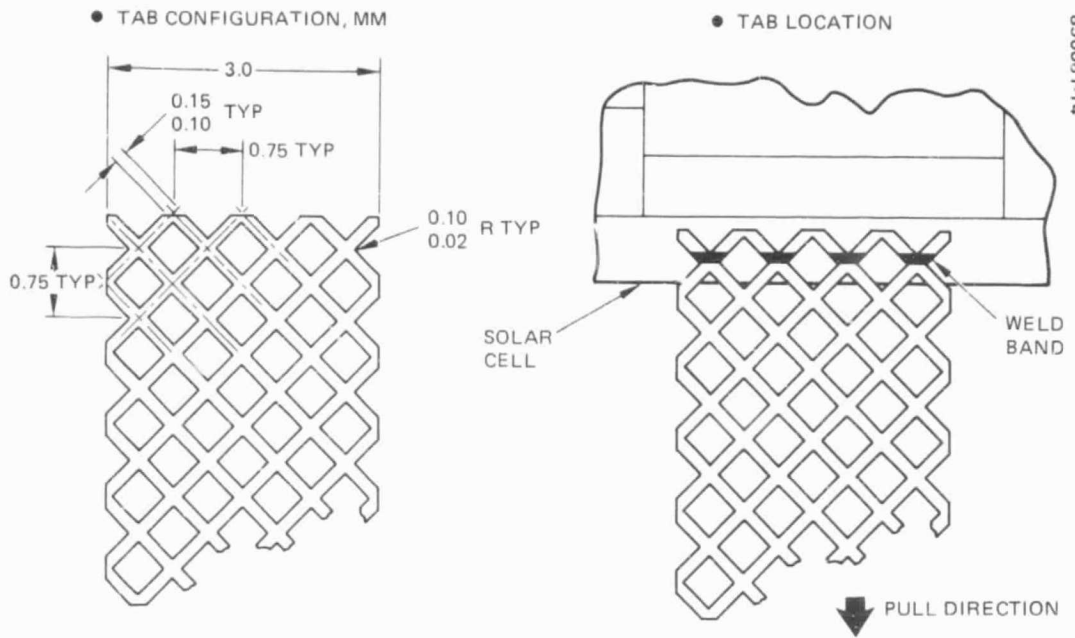


FIGURE 14. SCG PULL TAB CONFIGURATION

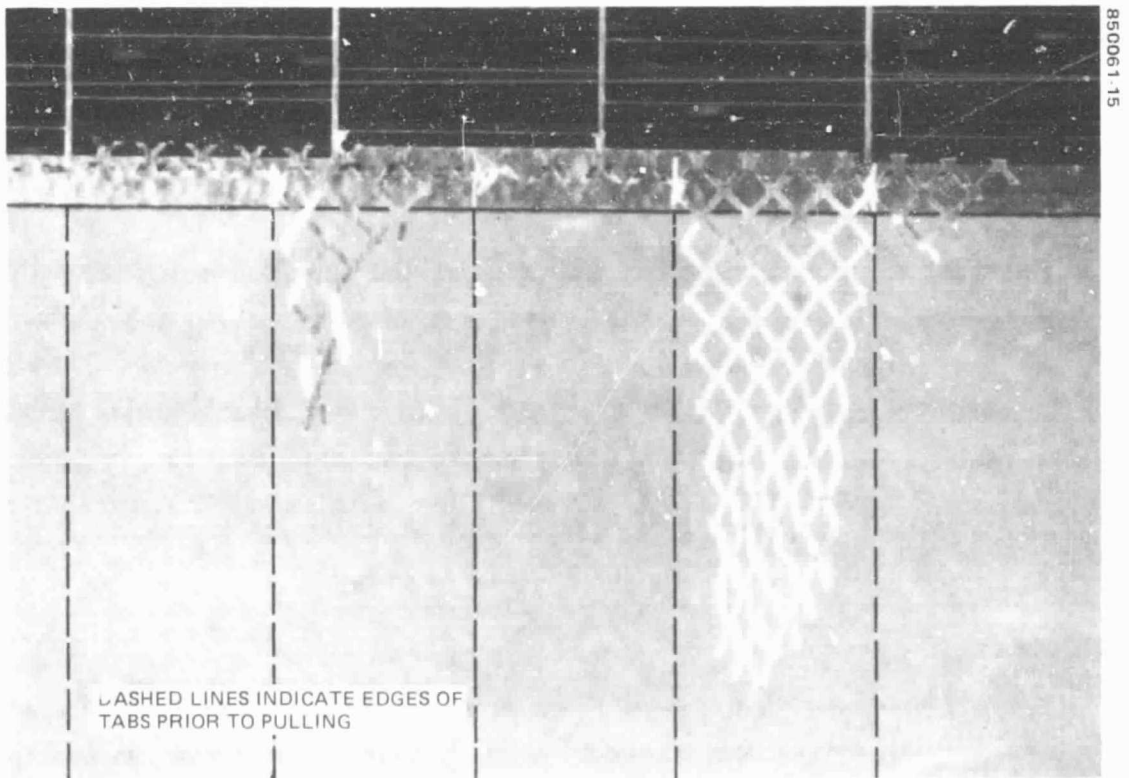


FIGURE 15. ULTRASONIC WELD PULL TABS

TABLE 5. PULL TEST OF ULTRASONIC BONDS\*

Parameter	At 45° Pull	At 90° Pull
Front		
Tabs tested	50	30
Tabs broken	50	26
Tab strength, gm	60 to 80	60 to 80
Welds separated	0	4
Separation force, gm	N/A	10 to 60
Back		
Tabs tested	30	10
Tabs broken	30	7
Tab strength, gm	60 to 80	60 to 80
Welds separated	0	3
Separation force, gm	N/A	20 to 40

\*Test with Unitron pull test machine.

TABLE 6. PULL TEST OF PARALLEL GAP BONDS\*

Parameter	At 45° Pull
Front Contact	
Tabs tested	14
Cells broken	5
Breaking force, gm	270 to 620
Welds separated	9
Separation force, gm	240 to 610
Back Contact	
Tabs tested	10
Cells broken	1
Breaking force, gm	400
Welds separated	9
Separation force, gm	240 to 500

\*Tested with Unitron pull test machine.

ORIGINAL PAGE IS  
OF POOR QUALITY.

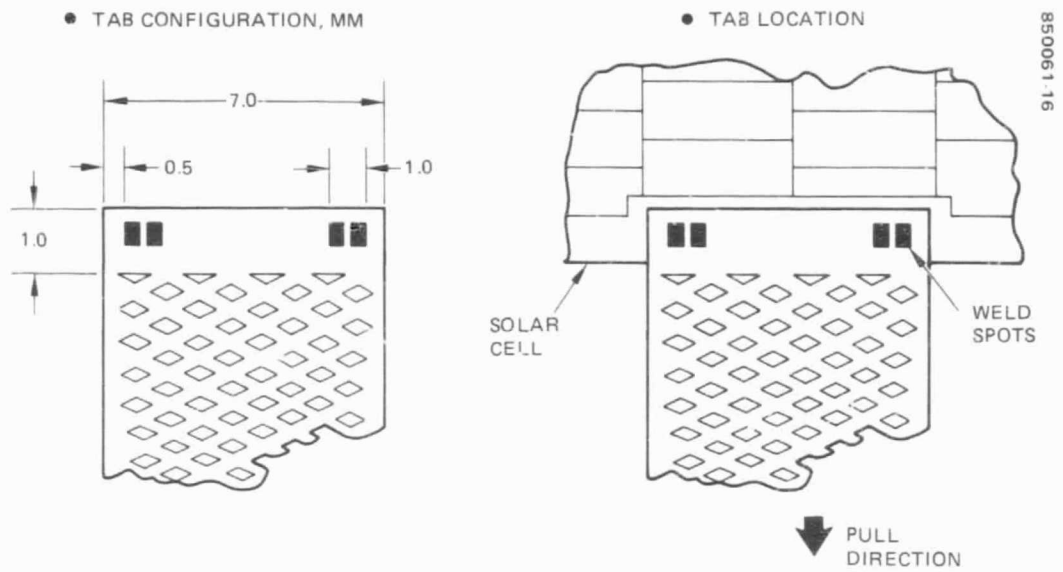


FIGURE 16. SPECTROLAB PULL TAB CONFIGURATION

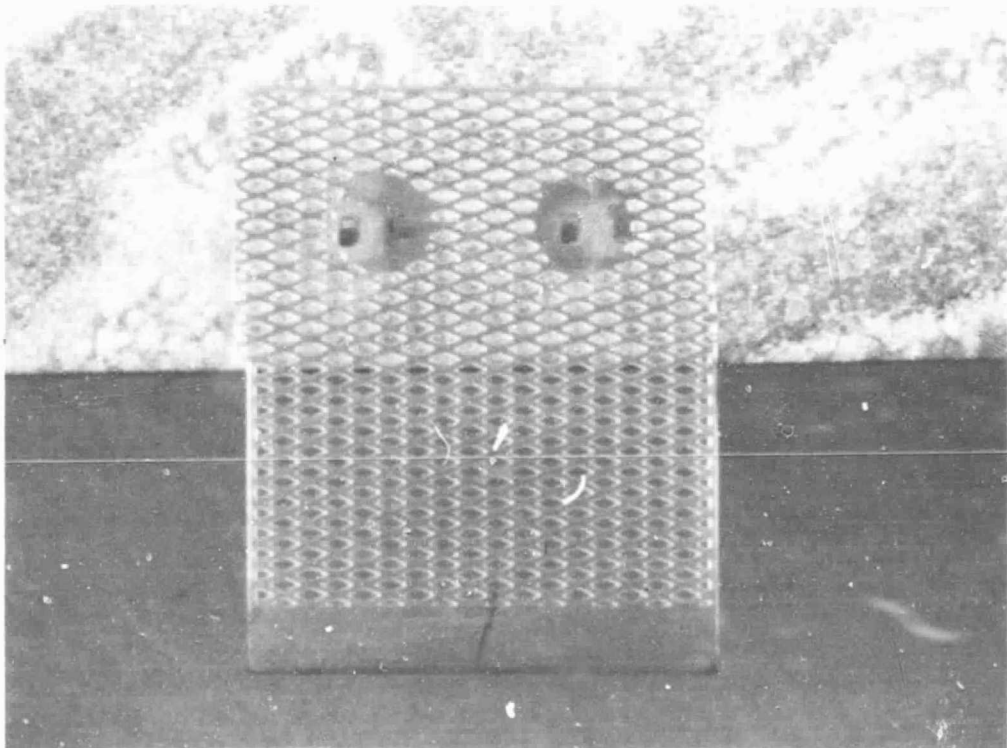


FIGURE 17. PARALLEL GAP WELD PULL TAB

request. Half of each type was welded at SCG, the other half at Spectrolab. Each cell assembly coupon comprised a covered cell which had interconnects welded to both the P and the N contacts, bonded to a segment of substrate. Each cell coupon consisted of an uncovered cell assembly coupon with interconnects welded to both the P and the N contacts, bonded to a segment of substrate. Examples are shown in Figures 18 and 19, prior to bonding to the substrate to depict the location of the welds on both the front and back of the cells.

ORIGINAL PAGE IS  
OF POOR QUALITY

850061-18

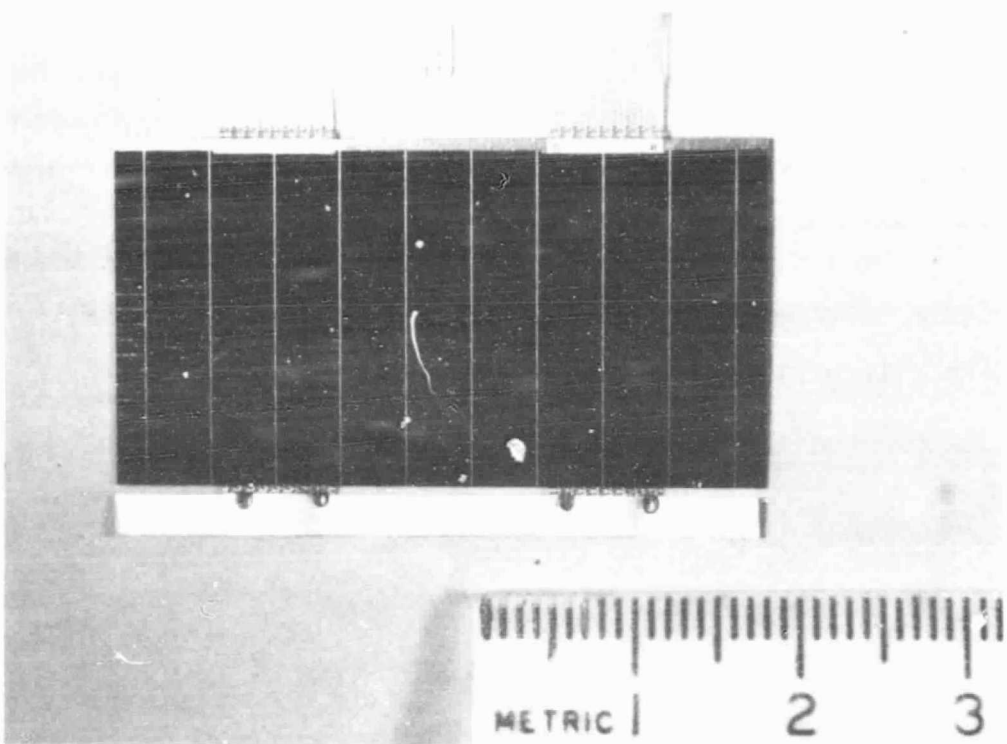


FIGURE 18. PARALLEL GAP WELDED CELL FRONT

850061-19

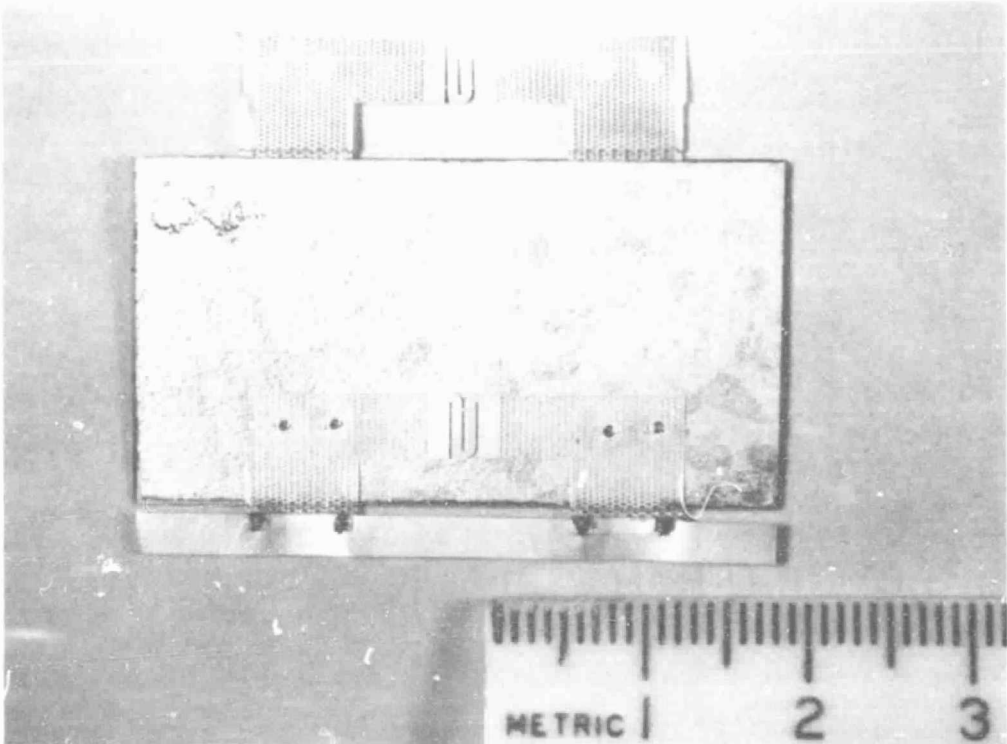


FIGURE 19. PARALLEL GAP WELDED CELL BACK

### 3. THERMAL TESTING

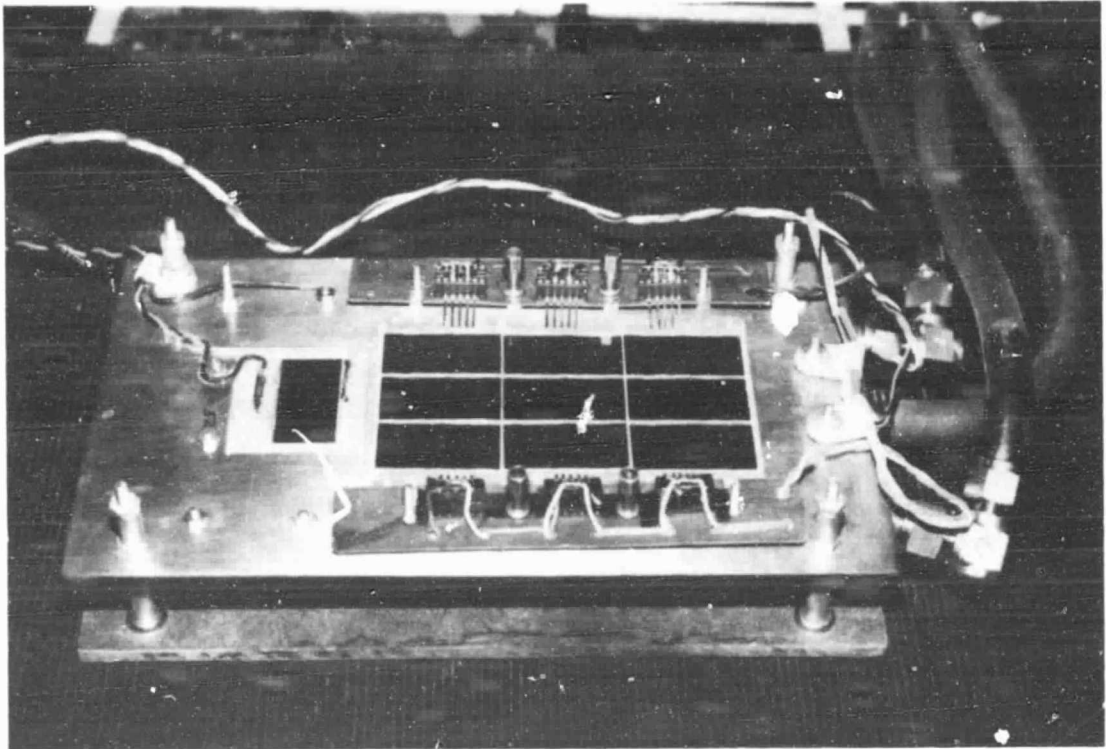
Twelve modules were thermally cycled: 4 ultrasonic welded (SCG), 4 parallel gap welded (Spectrolab), 2 SCG and 2 Spectrolab soldered. Two additional modules were used as noncycled control modules. Although not cycled, their electrical performance was measured each time performance was measured for the cycled cells. These control modules thereby served as a verification that electrical measurements were made in the same manner each time even though several months elapsed between measuring times.

Prior to starting the thermal cycling, all modules were examined optically (at 10x) and anomalies were recorded. The full current voltage photovoltaic output curve for each module at 28°C under air mass zero illumination also was recorded. For these measurements, each module was held by vacuum against a temperature controlled plate, as shown in Figure 20. A reference cell was mounted permanently on this plate to verify the level of illumination; two thermocouples verified the temperature of the plate.

These photovoltaic measurements and optical examinations were repeated after cycle 500, 1,000, 2,000, 4,000, 12,000, 18,000, 24,000, 30,000, and 36,000. To make these measurements, the cycling apparatus was stopped, the module tray disassembled, and current-voltage measurements were repeated in the same manner as the precycling measurements.

Photovoltaic measurements also were made at 80°C before starting the thermal cycling and then again after 12,000, 18,000, 24,000, 30,000, and 36,000 cycles. These higher temperature measurements were undertaken on the assumption that they provide a more sensitive means of early detection of incipient failure. Expansion of the adhesive between the cover and the cell would tend to pull the interconnect away from the cell. Thus, if a weld or solder joint had become loosened from thermal cycling, this high temperature expanded condition might have detected an open circuit whereas measurement

ORIGINAL PAGE IS  
OF POOR QUALITY



850061-20

FIGURE 20. SUNLIGHT SIMULATION TESTING MODULE FIXTURE

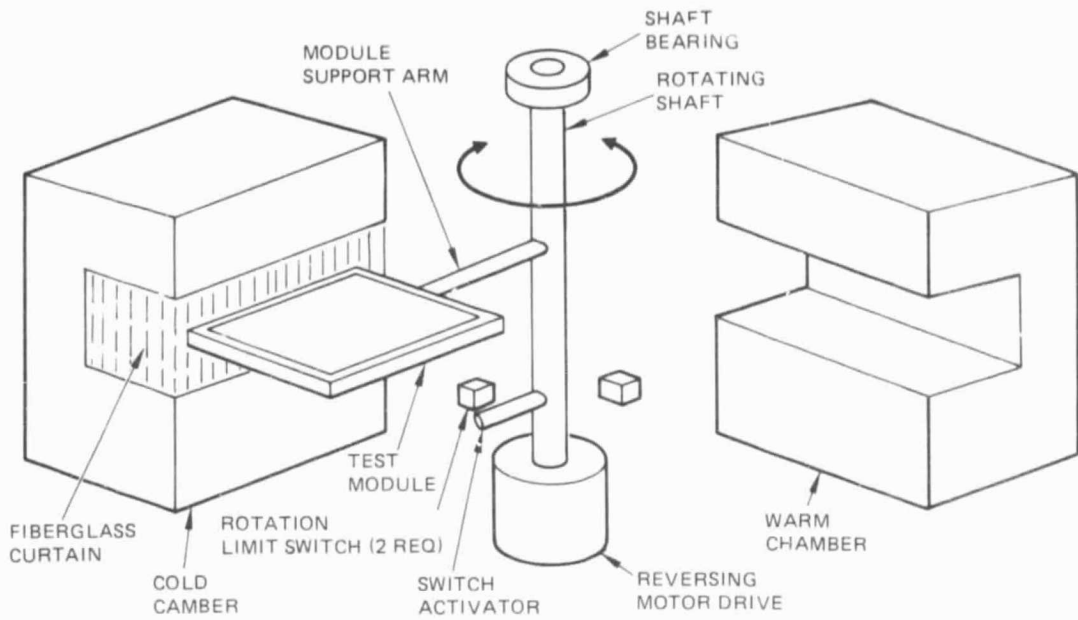


at 28°C would not if the interconnect at this lower temperature remained touching but was otherwise unbonded from its cell. These measurements at 80°C were made with an illumination several percent higher than AM0 in order to exaggerate any changes in series resistance.

To accomplish the thermal cycling, the 12 modules were supported on an aluminum tray stack that moved alternately from a warm chamber to a cold chamber at the rate of approximately one cycle every 10 minutes. The mechanism is enclosed within a housing that maintains a dry nitrogen gas environment. The mechanism is shown schematically in Figure 21. The housing, with its doors open to reveal the mechanism, is shown photographically in Figure 22. After loading the test tray, the doors of the housing were closed. The housing then was purged with dry nitrogen gas to remove all water vapor prior to starting the thermal cycling. A positive pressure of nitrogen was maintained throughout the cycling to ensure that no water or frost ever condensed on the modules.

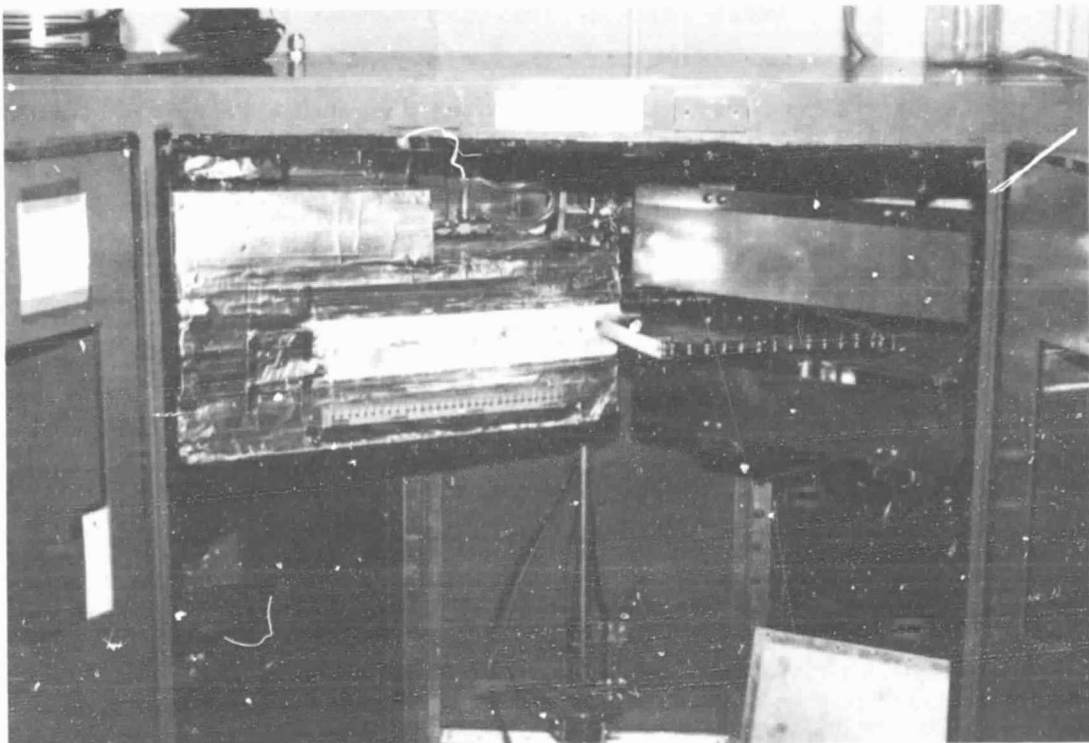
The tray stack consisted of four sheets of aluminum. The center two sheets each supported six modules; the outer two aided in providing a uniform temperature distribution across the entire area of the stack. This arrangement is depicted schematically in Figures 23 and 24, photographically in Figure 25. The modules were held in tension by metal coil springs attached along their edges, thus preventing curling of the modules during the alternating expansion and contraction of each cycle. A leaf spring of low thermal conductance held a low mass thermocouple against the center cell of each module. A small amount of thermally conductive compound (Dow Corning 340 silicone heat sink compound) was used to ensure the thermocouple was at the same temperature as the module. This compound retains its greaselike consistency over the temperature range of this test. It was easy to remove the compound from the modules every time the module tray was removed from cycling to make the periodic current-voltage measurements. The tray also contained additional thermocouples located so as to detect any undesired thermal gradients. The temperatures of all thermocouples were recorded periodically to form a record of module temperatures. Uniformity of  $\pm 5^{\circ}\text{C}$  over all modules was specified by NASA at both  $+80^{\circ}\text{C}$  and  $-80^{\circ}\text{C}$ . In practice, uniformity at the high temperature limit usually was within  $\pm 3^{\circ}\text{C}$ , at the low temperature within  $\pm 4^{\circ}\text{C}$ . On rare occasions, the temperature set limits drifted up or down a couple of degrees when operating automatically over an evening or weekend. While this led to a

ORIGINAL PAGE IS  
OF POOR QUALITY



850061 21

FIGURE 21. THERMAL CYCLING EQUIPMENT SCHEMATIC



850061 22

FIGURE 22. THERMAL CYCLING MACHINE

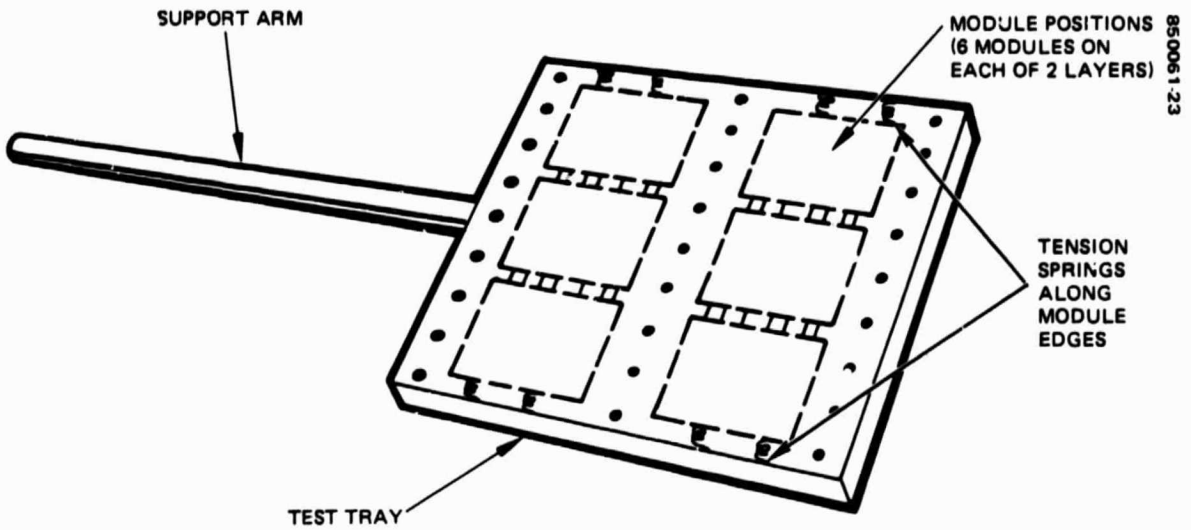


FIGURE 23. MODULE TEST TRAY

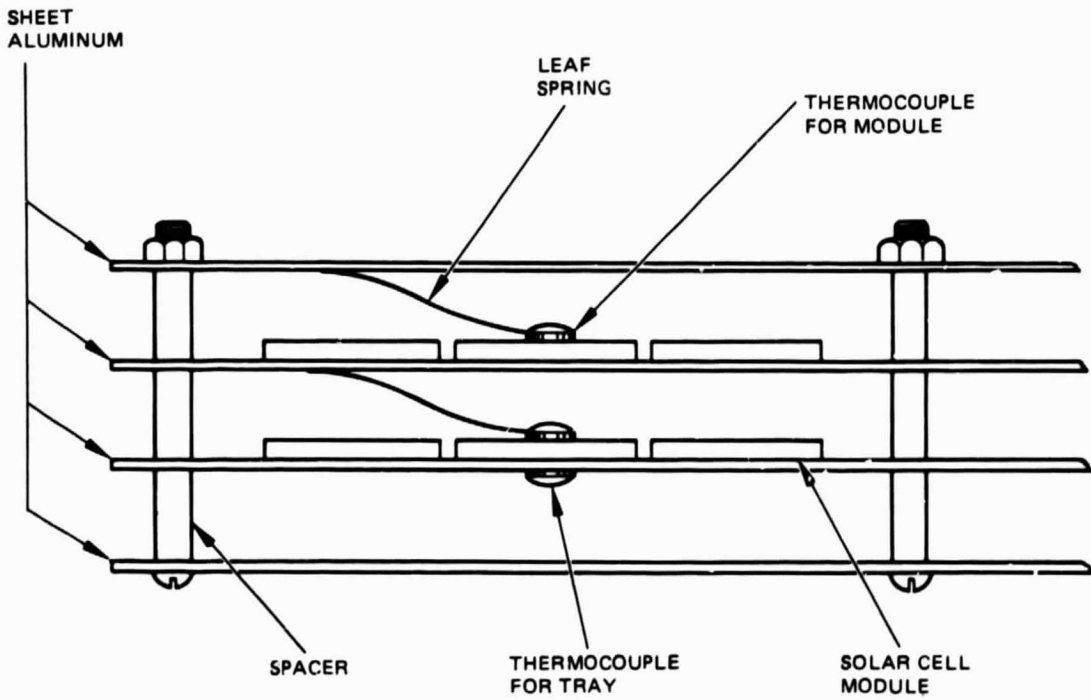


FIGURE 24. MODULE TEST TRAY CROSS SECTION

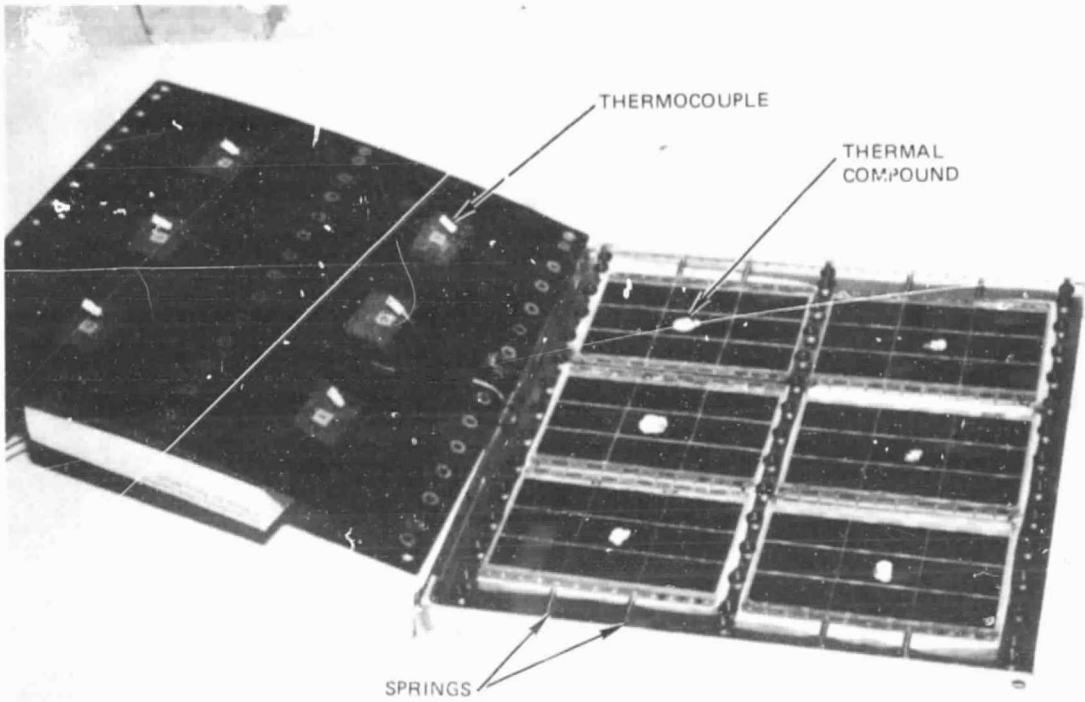


FIGURE 25. PARTIALLY ASSEMBLED MODULE TRAY

temporary excess of a degree or two beyond the nominal  $\pm 5^{\circ}\text{C}$  limit, such drifts affected both the low and high limits in the same direction so that the total swing in temperature remained close to  $160^{\circ}\text{C}$ .

The visual examinations and electrical measurements made periodically during this cycling test did not reveal any large changes. The only change noted visually was a slight roughening of the solder surface on some of the soldered cells after 8,000 cycles. There was no evidence that this roughened condition led to any performance degradation. The power output at AM0 illumination and  $28^{\circ}\text{C}$  remained unchanged.

The most likely electrical damage to search for on a thermally cycled module would be an increase of series resistance or a decrease in shunting resistance. Slight changes in either would manifest themselves as a change in the fill factor of the current-voltage curves for the modules. Table 7 shows there has been no change in fill factor at  $28^{\circ}\text{C}$ . Table 8 shows there also was little, if any, change in the fill factor at  $80^{\circ}\text{C}$  under measurement conditions that should have exaggerated such change. Interpreting these high temperature measurements with precision is difficult since  $80^{\circ}\text{C}$  was near the upper limit readily achievable with the test fixture shown in Figure 20. The data of Table 8 therefore may have more experimental scatter than that of Table 7. Only the soldered Spectrolab cells show any suggestion of possible degradation. However, measurement of these modules at high temperature was particularly difficult since the configuration of the electrical pressure contacts on the test fixture was not as compatible with the contacting pad configuration of these particular modules as they were with the pads on the other modules. Before concluding that an electrical degradation has been started on these soldered modules, thermal cycling would need to be extended well beyond the present 36,000 cycles to see if the fill factor established a more clearly defined downward trend or merely fluctuated from measurement to measurement because of measurement difficulty.

TABLE 7. FILL FACTORS AT 28°C FOR 12 MODULES DURING THERMAL TEST\*

Cycle	Ultrasonic Weld (Hughes)			Parallel Gap Weld (Spectrolab)				Solder (Hughes)		Solder (Spectrolab)		
	H2W	H7W	H11W	H12W	S1W	S2W	S4W	S5W	H8S	H10S	S7S	S10S
0	0.78	0.78	0.78	0.77	0.78	0.78	0.78	0.77	**	0.78	0.78	0.78
500	0.78	0.78	0.78	0.78	0.78	0.78	0.77	0.78	0.78	0.78	0.77	0.78
1,000	0.78	0.79	0.78	0.78	0.78	0.78	0.78	0.77	0.77	0.78	0.77	0.78
2,000	0.77	0.78	0.78	0.78	0.78	0.78	0.78	0.77	0.77	0.77	0.78	0.78
4,000	0.78	0.79	0.78	0.77	0.78	0.78	0.77	0.78	0.78	0.78	0.77	0.77
8,000	0.78	0.78	0.78	0.77	0.78	0.78	0.77	0.77	0.78	0.78	0.77	0.78
12,000	0.78	0.78	0.78	0.77	0.77	0.77	0.77	0.77	0.78	0.78	0.76	0.78
18,000	0.79	0.78	0.78	0.78	0.78	0.78	0.78	0.77	0.78	0.78	0.77	0.77
24,000	0.78	0.78	0.78	0.77	0.77	0.78	0.77	0.77	0.77	0.77	0.77	0.78
30,000	0.78	0.78	0.78	0.78	0.78	0.78	0.77	0.77	0.77	0.77	0.77	0.77
35,000	0.78	0.78	0.78	0.78	0.78	0.78	0.77	0.76	0.76	0.78	0.77	0.77

\*Fill factor  $\frac{\text{Max Power}}{I_{SC} \times V_{OC}}$  at AMO, 28°C.

\*\*Module H8S was not placed into the test until cycle 501; hence, it has 500 fewer cycles than the other modules at each inspection.

TABLE 8. FILL FACTORS AT 80°C FOR 12 MODULES DURING THERMAL TEST\*

Cycle	Ultrasonic Weld (Hughes)			Parallel Gap Weld (Spectrolab)				Solder (Hughes)		Solder (Spectrolab)		
	H2W	H7W	H11W	H12W	S1W	S2W	S4W	S5W	H8S	H10S	S7S	S10S
0	0.72	0.72	0.71	0.72	0.72	0.72	0.72	0.72	**	N/A	0.72	0.72
12,000	0.71	0.72	0.72	0.71	0.71	0.71	0.71	0.70	0.70	0.72	0.69	0.71
18,000	0.72	0.72	0.72	0.71	0.71	0.71	0.71	0.71	0.70	0.72	0.69	0.70
24,000	0.72	0.72	0.72	0.72	0.72	0.72	0.72	0.72	0.73	0.68	0.72	0.68
30,000	0.72	0.71	0.71	0.70	0.70	0.70	0.71	0.71	0.71	0.71	0.68	0.68
36,000	0.73	0.74	0.72	0.72	0.73	0.73	0.72	0.72	0.72	0.72	0.68	0.72

\*Fill factor  $\frac{\text{Max Power}}{I_{sc} \times V_{oc}}$  at AMO, 80°C.

\*\*Module H8S was not placed into the test until cycle 501; hence, it has 500 fewer cycles than the other modules at each inspection.

#### 4. CONCLUSION

These tests have indicated that solar array modules constructed with state of the art components and materials are able to withstand at least 6 years equivalent of near earth orbit thermal cycling without fatigue induced degradation of power.

PRECEDING PAGE BLANK NOT FILMED



## 5. NEW TECHNOLOGY

No items of new technology have been identified by Hughes Aircraft Company under this contract.

PRECEDING PAGE BLANK NOT FILMED